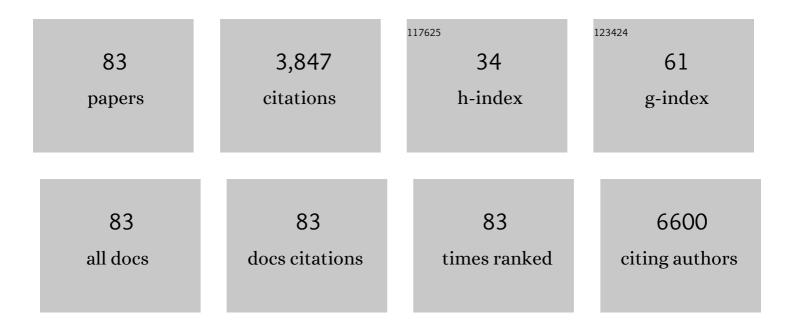
List of Publications by Year in descending order

Source: https://exaly.com/author-pdf/10513989/publications.pdf Version: 2024-02-01



#	Article	IF	CITATIONS
1	Metallic <i>vs.</i> semiconducting properties of quasi-one-dimensional tantalum selenide van der Waals nanoribbons. Nanoscale, 2022, 14, 6133-6143.	5.6	10
2	One-dimensional van der Waals quantum materials. Materials Today, 2022, 55, 74-91.	14.2	49
3	Tuning Spin Transport in a Graphene Antiferromagnetic Insulator. Physical Review Applied, 2022, 18, .	3.8	1
4	Vibronic Exciton–Phonon States in Stack-Engineered van der Waals Heterojunction Photodiodes. Nano Letters, 2022, 22, 5751-5758.	9.1	6
5	Electron transport through antiferromagnetic spin textures and skyrmions in a magnetic tunnel junction. Physical Review B, 2020, 102, .	3.2	7
6	High-frequency current oscillations in charge-density-wave 1T-TaS2 devices: Revisiting the "narrow band noise―concept. Applied Physics Letters, 2020, 116, .	3.3	15
7	Synthetic antiferromagnet-based spin Josephson oscillator. Applied Physics Letters, 2020, 116, 132409.	3.3	5
8	Growth of High-Quality Hexagonal Boron Nitride Single-Layer Films on Carburized Ni Substrates for Metal–Insulator–Metal Tunneling Devices. ACS Applied Materials & Interfaces, 2020, 12, 35318-35327.	8.0	7
9	Room-Temperature Electrodeposition of Aluminum via Manipulating Coordination Structure in AlCl3 Solutions. Journal of Physical Chemistry Letters, 2020, 11, 1589-1593.	4.6	18
10	Phonon and Thermal Properties of Quasi-Two-Dimensional FePS ₃ and MnPS ₃ Antiferromagnetic Semiconductors. ACS Nano, 2020, 14, 2424-2435.	14.6	58
11	Phononic and photonic properties of shape-engineered silicon nanoscale pillar arrays. Nanotechnology, 2020, 31, 30LT01.	2.6	12
12	Effects of filling, strain, and electric field on the Néel vector in antiferromagnetic CrSb. Physical Review B, 2020, 102, .	3.2	7
13	Growth Dynamics of Millimeter‧ized Singleâ€Crystal Hexagonal Boron Nitride Monolayers on Secondary Recrystallized Ni (100) Substrates. Advanced Materials Interfaces, 2019, 6, 1901198.	3.7	20
14	Bias-Voltage Driven Switching of the Charge-Density-Wave and Normal Metallic Phases in 1T-TaS ₂ Thin-Film Devices. ACS Nano, 2019, 13, 7231-7240.	14.6	57
15	A brain-plausible neuromorphic on-the-fly learning system implemented with magnetic domain wall analog memristors. Science Advances, 2019, 5, eaau8170.	10.3	56
16	Strain control of the Néel vector in Mn-based antiferromagnets. Applied Physics Letters, 2019, 114, .	3.3	20
17	Shape dependent resonant modes of skyrmions in magnetic nanodisks. Journal of Magnetism and Magnetic Materials, 2018, 455, 9-13.	2.3	19
18	Thermal Percolation Threshold and Thermal Properties of Composites with High Loading of Graphene and Boron Nitride Fillers. ACS Applied Materials & amp; Interfaces, 2018, 10, 37555-37565.	8.0	243

#	Article	IF	CITATIONS
19	Commensurate lattice constant dependent thermal conductivity of misoriented bilayer graphene. Carbon, 2018, 138, 451-457.	10.3	38
20	Long-distance spin transport through a graphene quantum Hall antiferromagnet. Nature Physics, 2018, 14, 907-911.	16.7	70
21	Interlayer transport through a graphene/rotated boron nitride/graphene heterostructure. Physical Review B, 2017, 95, .	3.2	12
22	Interlayer resistance of misoriented MoS ₂ . Physical Chemistry Chemical Physics, 2017, 19, 10406-10412.	2.8	12
23	Hot carrier-enhanced interlayer electron–hole pair multiplication in 2D semiconductor heterostructure photocells. Nature Nanotechnology, 2017, 12, 1134-1139.	31.5	74
24	Raman spectra of twisted CVD bilayer graphene. Carbon, 2017, 123, 302-306.	10.3	50
25	Phase Engineering of 2D Tin Sulfides. Small, 2016, 12, 2998-3004.	10.0	51
26	A charge-density-wave oscillator based on an integrated tantalum disulfide–boron nitride–graphene device operating at room temperature. Nature Nanotechnology, 2016, 11, 845-850.	31.5	170
27	Spin-Josephson effects in exchange coupled antiferromagnetic insulators. Physical Review B, 2016, 94, .	3.2	9
28	Direct observation of confined acoustic phonon polarization branches in free-standing semiconductor nanowires. Nature Communications, 2016, 7, 13400.	12.8	71
29	Uniform Benchmarking of Low-Voltage van der Waals FETs. IEEE Journal on Exploratory Solid-State Computational Devices and Circuits, 2016, 2, 28-35.	1.5	24
30	Fundamentals of lateral and vertical heterojunctions of atomically thin materials. Nanoscale, 2016, 8, 3870-3887.	5.6	117
31	Strong Circularly Polarized Photoluminescence from Multilayer MoS ₂ Through Plasma Driven Direct-Gap Transition. ACS Photonics, 2016, 3, 310-314.	6.6	12
32	Topological spin Hall effect resulting from magnetic skyrmions. Physical Review B, 2015, 92, .	3.2	53
33	Acoustic phonon spectrum and thermal transport in nanoporous alumina arrays. Applied Physics Letters, 2015, 107, .	3.3	35
34	Two step growth phenomena of molybdenum disulfide–tungsten disulfide heterostructures. Chemical Communications, 2015, 51, 11213-11216.	4.1	21
35	Theoretical and experimental study of highly textured GaAs on silicon using a graphene buffer layer. Journal of Crystal Growth, 2015, 425, 268-273.	1.5	25
36	Direct Bandgap Transition in Many‣ayer MoS ₂ by Plasmaâ€Induced Layer Decoupling. Advanced Materials, 2015, 27, 1573-1578.	21.0	102

#	Article	IF	CITATIONS
37	Electronic and thermoelectric properties of van der Waals materials with ring-shaped valence bands. Journal of Applied Physics, 2015, 118, .	2.5	120
38	Effect of strain on the electronic and optical properties of Ge–Si dome shaped nanocrystals. Physical Chemistry Chemical Physics, 2015, 17, 2484-2493.	2.8	5
39	Skyrmion creation and annihilation by spin waves. Applied Physics Letters, 2015, 107, .	3.3	39
40	Electronic and thermoelectric properties of few-layer transition metal dichalcogenides. Journal of Chemical Physics, 2014, 140, 124710.	3.0	321
41	Effect of Random, Discrete Source Dopant Distributions on Nanowire Tunnel FETs. IEEE Transactions on Electron Devices, 2014, 61, 2208-2214.	3.0	19
42	Nanoscale phononic interconnects in THz frequencies. Physical Chemistry Chemical Physics, 2014, 16, 23355-23364.	2.8	8
43	Tin Disulfide—An Emerging Layered Metal Dichalcogenide Semiconductor: Materials Properties and Device Characteristics. ACS Nano, 2014, 8, 10743-10755.	14.6	449
44	Towards van der Waals Epitaxial Growth of GaAs on Si using a Graphene Buffer Layer. Advanced Functional Materials, 2014, 24, 6629-6638.	14.9	113
45	Interlayer magnetoconductance of misoriented bilayer graphene ribbons. Journal of Applied Physics, 2013, 114, .	2.5	5
46	Multi-state current switching by voltage controlled coupling of crossed graphene nanoribbons. Journal of Applied Physics, 2013, 114, 153710.	2.5	5
47	Tunneling spectroscopy of chiral states in ultra-thin topological insulators. Journal of Applied Physics, 2013, 113, 063707.	2.5	6
48	The coherent interlayer resistance of a single, rotated interface between two stacks of AB graphite. Applied Physics Letters, 2013, 103, 243114.	3.3	25
49	Graphene-based non-Boolean logic circuits. Journal of Applied Physics, 2013, 114, .	2.5	60
50	Charge Density Waves in Exfoliated Films of van der Waals Materials: Evolution of Raman Spectrum in TiSe ₂ . Nano Letters, 2012, 12, 5941-5945.	9.1	154
51	Monolayer \$hbox{MoS}_{2}\$ Transistors Beyond the Technology Road Map. IEEE Transactions on Electron Devices, 2012, 59, 3250-3254.	3.0	156
52	Current modulation by voltage control of the quantum phase in crossed graphene nanoribbons. Physical Review B, 2012, 86, .	3.2	16
53	Doping, Tunnel Barriers, and Cold Carriers in InAs and InSb Nanowire Tunnel Transistors. IEEE Transactions on Electron Devices, 2012, 59, 2996-3001.	3.0	17
54	Electronic states of Ge/Si nanocrystals with crescent-shaped Ge-cores. Journal of Applied Physics, 2012, 112, .	2.5	5

ROGER K LAKE

#	Article	lF	CITATIONS
55	Material Selection for Minimizing Direct Tunneling in Nanowire Transistors. IEEE Transactions on Electron Devices, 2012, 59, 2064-2069.	3.0	41
56	\$hbox{TiSi}_{2}\$ Nanocrystal Metal Oxide Semiconductor Field Effect Transistor Memory. IEEE Nanotechnology Magazine, 2011, 10, 499-505.	2.0	10
57	Effects of heavily doped source on the subthreshold characteristics of nanowire tunneling transistors. , 2011, , .		1
58	Negative differential resistance in bilayer graphene nanoribbons. Applied Physics Letters, 2011, 98, .	3.3	52
59	Permanent Electric Dipole Moments of Carboxyamides in Condensed Media: What Are the Limitations of Theory and Experiment?. Journal of Physical Chemistry B, 2011, 115, 9473-9490.	2.6	39
60	Hybrid Graphene Nanoribbon-CMOS tunneling volatile memory fabric. , 2011, , .		12
61	Carrier leakage in Ge/Si core-shell nanocrystals for lasers: core size and strain effects. Proceedings of SPIE, 2011, , .	0.8	3
62	Core size dependence of the confinement energies, barrier heights, and hole lifetimes in Ge-core/Si-shell nanocrystals. Journal of Applied Physics, 2011, 110, .	2.5	13
63	Effects of band-tails on the subthreshold characteristics of nanowire band-to-band tunneling transistors. Journal of Applied Physics, 2011, 110, .	2.5	54
64	Conductance switching in diarylethenes bridging carbon nanotubes. Journal of Chemical Physics, 2011, 134, 024524.	3.0	37
65	Diameter dependent performance of high-speed, low-power InAs nanowire field-effect transistors. Journal of Applied Physics, 2010, 107, 014502.	2.5	24
66	Modeling and performance analysis of GaN nanowire field-effect transistors and band-to-band tunneling field-effect transistors. Journal of Applied Physics, 2010, 108, 104503.	2.5	13
67	Performance analysis of InP nanowire band-to-band tunneling field-effect transistors. Applied Physics Letters, 2009, 95, 073504.	3.3	9
68	High-Speed and Low-Power Performance of n-type InSb/InP and InAs/InP Core/Shell Nanowire Field Effect Transistors for CMOS Logic Applications. Materials Research Society Symposia Proceedings, 2009, 1178, 26.	0.1	0
69	The Quantum and Classical Capacitance Limits of InSb and InAs Nanowire FETs. IEEE Transactions on Electron Devices, 2009, 56, 2215-2223.	3.0	23
70	Theoretical design of bioinspired macromolecular electrets based on anthranilamide derivatives. Biotechnology Progress, 2009, 25, 915-922.	2.6	23
71	Conductance of a conjugated molecule with carbon nanotube contacts. Physical Review B, 2009, 80, .	3.2	20
72	Modeling and performance analysis of high-speed, high-power GaN nanowire FETs. , 2009, , .		0

#	Article	IF	CITATIONS
73	Drive Currents and Leakage Currents in InSb and InAs Nanowire and Carbon Nanotube Band-to-Band Tunneling FETs. IEEE Electron Device Letters, 2009, 30, 1257-1259.	3.9	31
74	Performance of \$n\$-Type InSb and InAs Nanowire Field-Effect Transistors. IEEE Transactions on Electron Devices, 2008, 55, 2939-2945.	3.0	48
75	The quantum capacitance limit of high-speed, low-power InSb nanowire field effect transistors. , 2008, , .		5
76	Electron transport through a conjugated molecule with carbon nanotube leads. Physical Review B, 2007, 76, .	3.2	35
77	Electronic properties of carbon nanotubes calculated from density functional theory and the empirical π-bond model. Journal of Computational Electronics, 2007, 6, 395-400.	2.5	11
78	Carbon nanotube - molecular resonant tunneling diode. Physica Status Solidi (A) Applications and Materials Science, 2006, 203, R5-R7.	1.8	17
79	Self-Assembled Carbon Nanotubes for Electronic Circuit and Device Applications. Journal of Nanoelectronics and Optoelectronics, 2006, 1, 74-81.	0.5	7
80	Leakage and performance of zero-Schottky-barrier carbon nanotube transistors. Journal of Applied Physics, 2005, 98, 064307.	2.5	44
81	Interface effects in tunneling models with identical real and complex dispersions. Physical Review B, 1999, 59, 7316-7319.	3.2	1
82	Quantitative simulation of a resonant tunneling diode. Journal of Applied Physics, 1997, 81, 3207-3213.	2.5	139
83	Transmission resonances and zeros in multiband models. Physical Review B, 1995, 52, 2754-2765.	3.2	56